Potential Energy Curves for Cation−π Interactions: Off-Axis Configurations Are Also Attractive

4 AUTHORS, INCLUDING:

Michael Marshall
Georgia Institute of Technology
13 PUBLICATIONS **549** CITATIONS

SEE PROFILE

Sahan Thanthiriwatte
University of Alabama
17 PUBLICATIONS **456** CITATIONS

SEE PROFILE

Charles David Sherrill
Georgia Institute of Technology
174 PUBLICATIONS **10,260** CITATIONS

SEE PROFILE

Potential Energy Curves for Cation−π Interactions: Off-Axis Configurations Are Also Attractive

Michael S. Marshall, Ryan P. Steele,[†] Kanchana S. Thanthiriwatte, and C. David Sherrill*

Center for Computational Molecular Science and Technology, School of Chemistry and Biochemistry, Georgia Institute of Technology, Atlanta, Georgia 30332-0400

Received: June 29, 2009; Revised Manuscript Received: October 12, 2009

Accurate potential energy surfaces for benzene·M complexes (M = Li$^+$, Na$^+$, K$^+$, and NH$_4^+$) are obtained using coupled-cluster theory through perturbative triple excitations, CCSD(T). Our computations show that off-axis cation−π interactions, where the cation is not directly above the aromatic ring, can be favorable and may influence molecular recognition. Even perpendicular, side-on interactions retain 18−32% of their π-face interaction energy in the gas phase, making their bond strengths comparable to hydrogen bonds in the gas phase. Solvent effects have been explored for each complex using the polarizable continuum model.

I. Introduction

Cation−π interactions are one of the fundamental forces of molecular recognition,[1] and they have been implicated in a number of biochemical processes, including the binding of acetylcholine by various acetylcholine receptors, ion selectivity in K$^+$ channels, and steroid biosynthesis.[2−4] Meadows et al. estimate that 8% of protein residues are potentially involved in cation−π interactions.[5] The large number of cation−π interactions present in proteins argues for a more complete understanding of the nature of these interactions. Cation−π interactions have been the focus of a vast array of recent research efforts.[1,3,5−31]

The attraction between a cation and an aromatic ring can be quite strong. Although nonpolar, benzene can compete with a water molecule for binding a cation in the gas phase. For example, the interaction energy of benzene·K$^+$ is −18 kcal mol^{-1}, compared to −19 kcal mol^{-1} for K$^+$ (H$_2$O).[32] The experimental interaction energies of benzene·Na$^+$ and benzene·Li$^+$ are stronger still, at −22.13 ± 1.39 and −38.50 ± 3.23 kcal mol^{-1}, respectively.[23]

Understanding the nature of the cation−π interaction in model systems has been a topic of much recent interest. Earlier studies explained the strength of the cation−π interaction as arising primarily from the electrostatic attraction between an ion and the large quadrupole moment featured by many aromatic rings.[3] However, it is now clear that the induction term is at least as important as the electrostatic term.[13,14,33]

Very high level quantum mechanical computations on the prototype benzene·Na$^+$ complex have been reported by Feller,[25] who estimated interaction energies using coupled-cluster theory with perturbative triple excitations [CCSD(T)] and complete basis set (CBS) extrapolations. Feller's theoretical interaction energy ($\Delta H_0 = -24.4 \pm 0.3$ kcal mol^{-1}) falls between two experimental results (−21.1 and −27.6 kcal mol^{-1})[34] which differ by 6.5 kcal mol^{-1}. An additional high-level theoretical study by Feller et al.[35] for the complexes of alkali earth cations with benzene indicates that lower level computations can yield 298 K binding energies which are 3−4 kcal mol^{-1} too low.

Woolf and co-workers have found[36] that the CHARMM force field does not always reliably model the interaction of indoles with point charges when compared to the more reliable density functional theory (DFT).

The effect of substituents on cation−π interactions has been examined in several recent theoretical and experimental papers.[28,37−39] Electrostatic interactions appear to be sufficient to explain computed trends in substituent effects,[28,37,38] although Amunugama and Rodgers also point out the role of the polarizability of the aromatic.[37,38] The interaction of benzene with ions MX$^+$ has also been examined,[40] where M is an alkaline earth dication and X is a counterion (e.g., H$^-$, CH$_3^-$).

Despite the large number of recent studies on cation−π interactions, previous work focuses only on cations interacting directly with the face of the aromatic ring. This is rather surprising considering that many off-angle cation−π interactions have been found in proteins.[19,24,26,29] Because the geometry of cation−π interactions may be constrained when these interactions occur in larger chemical or biochemical systems, it is important to know how the attractions behave as a function of distance and orientation. While these interactions will certainly be attenuated in larger systems due to polarization of the environment, the gas-phase potential energy curves represent the first step in understanding the nature of the fundamental cation−π interaction. Moreover, they may serve as benchmarks in the development of the next generation of polarizable force fields which may accurately model noncovalent interactions in biochemical systems. In this work, we present high-level quantum mechanical computations of potential energy curves for cation−π interactions by considering complexes of the cations Li$^+$, K$^+$, Na$^+$, and NH$_4^+$ with benzene, and we include configurations in which the cation is not directly above the aromatic ring. Contrary to expectations based on electrostatic interactions alone, we find that off-axis approaches can be favorable—although not nearly as favorable as binding to the top of the ring—suggesting that off-axis cation−π interactions should also be considered when analyzing biochemical systems.

II. Theoretical Approach

Potential energy surfaces (PES) were computed using the CCSD(T) method[41] with the Pople 6-311++G(2d,2p) basis set.[42−44] All interaction energies were corrected for basis set

* To whom correspondence should be addressed. E-mail: sherrill@gatech.edu.
† Present address: Yale University, 225 Prospect Street, New Haven, CT 06520.
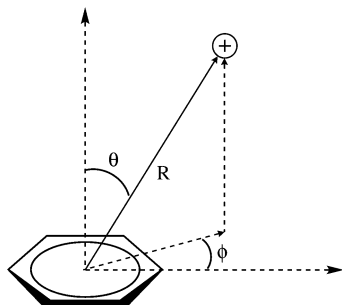
Potential Energy Curves for Cation−π Interactions

J. Phys. Chem. A, Vol. 113, No. 48, 2009 **13629**

Figure 1. Geometries for cation−π systems.

Figure 2. Potential energy curves for given (θ, ϕ) values for benzene·M$^+$ (M = Li, Na, K, NH$_4$) at the CCSD(T)/6-311++G(2d,2p) level of theory: (a) benzene·Li$^+$; (b) benzene·Na$^+$; (c) benzene·K$^+$; (d) benzene·NH$_4^+$.

superposition error (BSSE) using the scheme outlined by Boys and Bernardi.[45] All single-point energies had the following orbitals frozen for each atom: C[1s], Na[1s], K[1s,2s,2p], N[1s], and Li[none]. The curves were computed with rigid monomers employing the benzene geometry recommended by Gauss and Stanton: $r_{CC} = 1.3915$ Å and $r_{CH} = 1.0800$ Å.[46] The NH$_4^+$ geometry, $r_{NH} = 1.0235$ Å and $\theta_{HNH} = 109.467°$, was acquired from a full CCSD(T)/aug-cc-pVTZ optimization. The NH$_4^+$ is oriented such that only one hydrogen points to the center of the ring. Very small changes in the interaction energy are found for different orientations. Displacements for the PES are calculated from the center of mass of the benzene to the center of mass of the cation. Rigid PES scans were performed on a dense grid of points for $R \in [2.0$ Å, 7.0 Å $]$, $\theta \in [0°, 90°]$, and $\phi = 0$ or $30°$ (see Figure 1). All computations were carried out with the MOLPRO 2006 program.[47] Because we are tracing potential curves and because monomer geometries were frozen, the geometries considered do not represent stationary points on the potential surface. Hence, zero point corrections were not applied.

III. Results and Discussion

Cation−π Interactions. Potential energy surfaces for various metal cations and ammonium interacting with aromatic benzene are shown in Figure 2. Interaction energies for the minimum of each curve are given in Table 1. In each case, the most favorable geometry is one where the cation is directly above the ring ($\theta = \phi = 0°$). For this configuration, the equilibrium CCSD(T)/6-311++G(2d,2p) interaction energies are -35.8, -22.2, -16.5, and -16.4 kcal mol^{-1} for Li$^+$, Na$^+$, K$^+$, and NH$_4^+$, respectively. Our results for the cation above the ring ($\theta = 0°$) are in good agreement with the previous experimental work of Amicangelo and Armentrout,[23] who report interaction energies of -38.5, -22.1, and -17.5 kcal mol^{-1} for Li$^+$, Na$^+$, and K$^+$, respectively, even though our results are purely electronic binding energies, neglecting enthalpy corrections. Our results are slightly less bound than the very high quality CCSD(T) complete-basis-set estimates of Feller et al.,[35] who obtain electronic interaction energies of -38.0, -25.4, and -20.6 kcal mol^{-1} for Li$^+$, Na$^+$, and K$^+$. We attribute the differences primarily to remaining deficiencies in the basis set and to the lack of geometry relaxation in our results (full geometry relaxation is somewhat more important for these cation−π interactions than for neutral noncovalent interactions, and it can be as large as ~1.5 kcal mol^{-1} for benzene·Li$^+$).

As the cation is moved from above the aromatic face ($\theta = 0°$) to the side-on geometry ($\theta = 90°$), we see that up to 30% of its interaction energy is retained, meaning the side-on interactions are still significantly stabilized (-11.33, -5.13, -2.96, and -3.38 kcal mol^{-1} for Li$^+$, Na$^+$, K$^+$, and NH$_4^+$, respectively, at the optimum values of R). The side-on geom-

etries are saddle points, rather than local minima, on the gas-phase potential energy surface. Nevertheless, side-on or near-side-on geometries can occur in complex environments such as proteins due to backbone or other steric constraints. Although the gas-phase interaction energies would be reduced in solution, their large magnitude indicates that even side-on interactions may be important in molecular recognition.
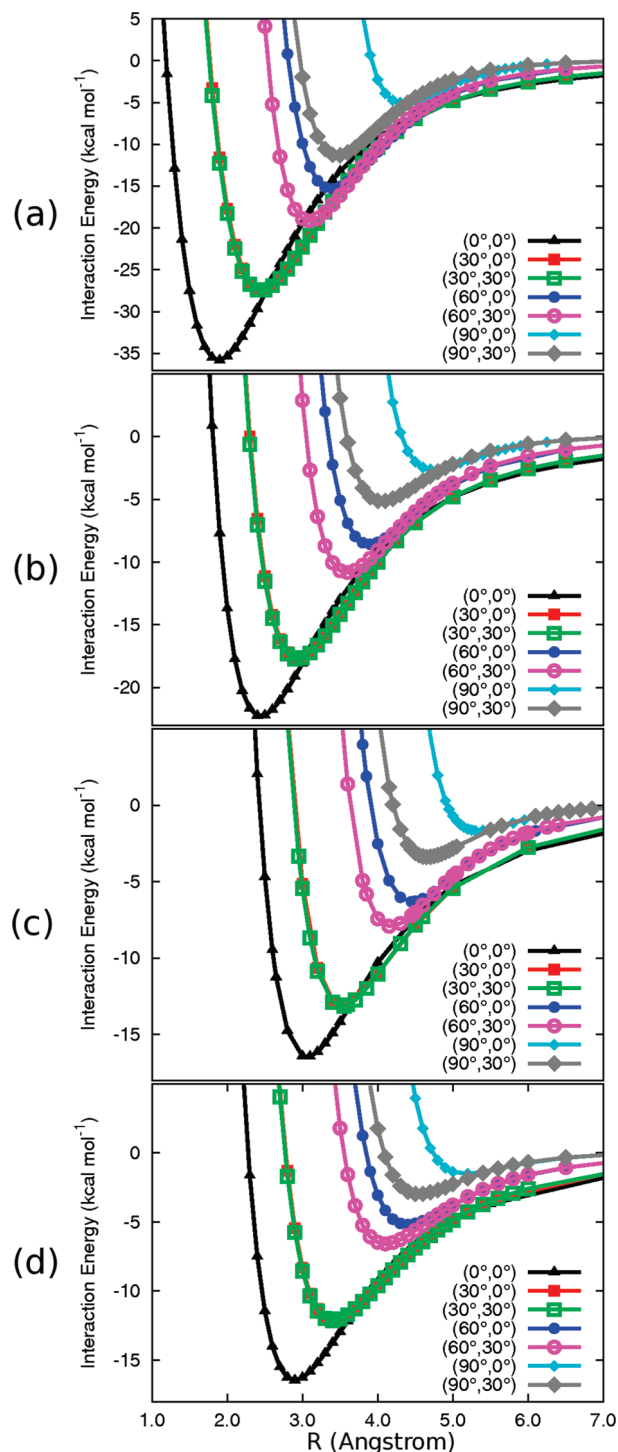
For all configurations where the cation is not directly above the benzene, there was a clear preference for $\phi = 30°$ (where the cation is positioned between two H atoms) over $\phi = 0°$

TABLE 1: CCSD(T)/6-311++G(2d,2p) Counterpoise Corrected Interaction Energies (E_{int}, kcal mol^{-1}) and Equilibrium Distances (R, Å)

cation	θ	ϕ	E_{int}	R
Li$^+$	0	0	−35.8	1.9
	30	0	−27.3	2.5
	60	0	−15.3	3.4
	90	0	−5.0	4.3
	30	30	−27.4	2.4
	60	30	−19.2	3.1
	90	30	−11.3	3.5
Na$^+$	0	0	−22.2	2.4
	30	0	−17.6	2.9
	60	0	−8.6	3.9
	90	0	−2.6	4.7
	30	30	−17.7	2.9
	60	30	−10.8	3.6
	90	30	−5.1	4.1
K$^+$	0	0	−16.5	2.9
	30	0	−12.1	3.4
	60	0	−5.2	4.4
	90	0	−1.5	5.2
	30	30	−12.1	3.4
	60	30	−6.6	4.1
	90	30	−3.0	4.5
NH$_4^+$	0	0	−16.4	3.1
	30	0	−13.0	3.6
	60	0	−6.3	4.5
	90	0	−1.7	5.3
	30	30	−13.1	3.6
	60	30	−7.9	4.2
	90	30	−3.4	4.6

(where the cation is aligned in a vertical plane with an H atom; see Figure 1). Our results indicate that the size of the cation plays a substantial role in its interaction energy. As size of the cation increases, the interaction energy decreases. This is primarily due to the significant role of induction. The small cations can approach closer to the ring and therefore can induce a much larger polarization response from the benzene. Supporting Information Figure 1 compares the potential energy curves for the side-on configurations ($\theta = 90°$, $\phi = 30°$) for the various cations considered. The curves for Na$^+$, K$^+$, and NH$_4^+$ are similar, but Li$^+$ is significantly more bound because of its smaller size.

Decomposition of Na$^+$−π Interaction Energy. To better understand how the cation−π interaction changes from in-plane ($\theta = 90°$, $\phi = 30°$) to above the π-face ($\theta = 0°$, $\phi = 0°$), we utilize density functional based symmetry adapted perturbation theory (DFT-SAPT)[48] to examine benzene·Na$^+$ as a representative example. DFT-SAPT is a recent extension of SAPT[49,50] theory where the interacting monomers are expressed in terms of Kohn−Sham DFT. DFT-SAPT has been shown to accurately reproduce coupled-cluster interaction energies.[51] To achieve such accuracy, one must asymptotically correct the exchange-correlation functional.[52−54] In this work we employ the gradient-regulated asymptotic correction of Grüning et al.[55] The shift parameters used for benzene and Na$^+$ are 0.0713 and 0.2783 hartree, respectively. These values are calculated from the difference between the HOMO energy and the exact ionization potential of each monomer. The exact ionization potentials are taken from Cohen and Taylor[56] for Na$^+$ (47.2864 eV) and Lias[57] for benzene (9.2459 eV). All DFT-SAPT calculations were carried out with the MOLPRO 2006 program[47] using the PBE0 density functional[58] and the 6-311++G(2d,2p)[42−44] basis set.

Within the DFT-SAPT framework, the interaction energy is decomposed into the following contributions: electrostatics,

induction, exchange, and dispersion. The total interaction energy can be defined as follows:

$$E_{interaction}^{DFT-SAPT} = E_{elst}^{(1)} + E_{exch}^{(1)} + E_{ind}^{(2)} + E_{exch-ind}^{(2)} + E_{disp}^{(2)} + E_{exch-disp}^{(2)} \quad (1)$$

The superscripts refer to the order of the correction. As done in our previous studies and by others,[6,59] we collect energy components as follows:

$$E_{ind} = E_{ind}^{(2)} + E_{exch-ind}^{(2)} \quad (2)$$

$$E_{disp} = E_{disp}^{(2)} + E_{exch-disp}^{(2)} \quad (3)$$

which results in an total interaction energy of

$$E_{total} = E_{exch}^{(1)} + E_{elst}^{(1)} + E_{disp} + E_{ind} \quad (4)$$

Using the methods and decomposition scheme outlined above, the energetic contributions for the above-face and in-plane configurations are computed for benzene·Na$^+$ (Supporting Information Figure 2). For the cation above the π-face, the interaction is equally stabilized by electrostatics (47%) and induction (49%), with dispersion only contributing 4% of the stabilizing interaction. Both CCSD(T) and DFT-SAPT predict that the in-plane configuration are bound. With the exception of the small contribution of dispersion, the in-plane configuration is entirely bound by induction. The electrostatic term for the in-plane configuration is repulsive because the closest contacts are between the cation and two hydrogens of benzene, which have partial positive charges. Most likely this is the reason earlier studies disregarded these configurations. To validate the reliability of DFT-SAPT for cation−π interactions, we compare DFT-SAPT to the published SAPT data of Soteras et al.[13] for the case of Na$^+$ above benzene (see Supporting Information Figure 3). Note also how well the interaction energy predicted by DFT-SAPT (−4.9 kcal mol^{-1}) compares to CCSD(T) (−5.1 kcal mol^{-1}).

Solvent Effects. Solvent effects on the strength of the cation−π interactions were examined with polarized continuum model (PCM)[60−63] using the B3LYP[64] density functional and the 6-311++G(2d,2p) basis set. All solvent calculations were performed using the GAMESS program.[65] The CCSD(T) interaction energies were corrected by adding the solvent free energy of interaction (ΔG_{solv}^{int}) using eqs 5 and 6.

$$E_{total}^{solv-int} = E_{CCSD(T)}^{int} + \Delta G_{solv}^{int} \quad (5)$$

where

$$\Delta G_{solv}^{int} = \Delta G_{solv}^{AB} - \Delta G_{solv}^{A} - \Delta G_{solv}^{B} \quad (6)$$

Three configurations were considered for each cation−benzene complex [$\theta, \phi = (0,0)$, $(60,30)$, and $(90,30)$] and R taken from equilibrium distance computed using the CCSD(T)/6-311++G(2d,2p) level of theory. Interaction energies were computed for water ($\epsilon = 78.39$) and chloroform ($\epsilon = 4.9$). Chloroform was chosen because it has a dielectric constant

Potential Energy Curves for Cation−π Interactions

J. Phys. Chem. A, Vol. 113, No. 48, 2009 **13631**

TABLE 2: Solvated Interaction Energies (kcal mol^{-1})^a

cation	θ	ϕ	R (Å)	interaction energy		
				gas phase	chloroform	water
Li$^+$	0	0	1.9	−35.8	−21.2	−18.4
	60	30	3.1	−19.2	−8.0	−6.0
	90	30	3.5	−11.3	0.7	−0.7
Na$^+$	0	0	2.4	−22.2	−15.1	−14.4
	60	30	3.6	−10.8	−4.8	−4.2
	90	30	4.1	−5.1	0.4	0.9
K$^+$	0	0	2.9	−16.5	−9.2	−8.5
	60	30	4.1	−6.6	−1.2	−0.8
	90	30	4.5	−3.0	1.5	1.6
NH$_4^+$	0	0	3.1	−16.4	−2.6	−0.4
	60	30	4.2	−7.9	2.3	3.6
	90	30	4.6	−3.4	3.9	4.6

^{a} Gas phase computed at CCSD(T)/6-311++G(2d,2p). Solvation correction computed at B3LYP-PCM/6-311++G(2d,2p).

closer to what one would find in the interior of a protein.[66] Solvated interaction energies are shown in Table 2. While the cation−π interactions are indeed attenuated by solvent, they can still be favorable, even for some of the off-axis configurations.

Comparison to Lower Levels of Theory. Considering that lower levels of theory have been popular for studies of cation−π interactions,[12,16,31] it is useful to evaluate the reliability of more approximate methods for these systems. Møller−Plesset perturbation theory (MP2; see Supporting Information Figure 4) and Hartree−Fock self-consistent-field (SCF; see Supporting Information Figure 5) are compared to CCSD(T). Out of the geometries considered above, this analysis included all points where both levels of theory predicted binding. MP2 interaction energies are comparable to CCSD(T) with a root-mean-square deviation (rmsd) of only 0.43 kcal mol^{-1} (maximum deviation of 2.58 kcal mol^{-1}). SCF, on the other hand, has a rmsd = 1.25 kcal mol^{-1} (maximum deviation of 6.52 kcal mol^{-1}). SCF does not include dynamical electron correlation; therefore, it fails to describe dispersion interactions. While not as dominant as the electrostatic and induction contributions, the dispersion term is expected to account for 2, 6, and 16% of the attractive interactions for Li$^+$−, Na$^+$−, and K$^+$−benzene complexes (where the cation is directly above the π-face), respectively.[13] If MP2 or CCSD(T) are not computationally affordable, the inclusion of an empirical dispersion term should be considered for methods such as SCF or DFT. Density-fitted MP2 (DF-MP2) has also been shown to be a very good substitute for MP2 for cation−π interactions.[18]

IV. Conclusions

To our knowledge, this work is the first to present potential energy surfaces for cation−π interactions where the cation is not necessarily above the center of the aromatic ring. Our computations at the CCSD(T)/6-311++G(2d,2p) level of theory show that even in-plane cation−π interactions can be favorable, with gas-phase interaction energies of −3 to −11 kcal mol^{-1} for the systems considered here. These off-axis interactions are not as strong as those directly above the ring face but are still near the strength of hydrogen bonds in the gas phase. Thus, we believe that the concept of a cation−π interaction should be broadened to include configurations where the cation may not be directly above the aromatic ring (and may even be in the same plane). PCM computations of solvent effects indicate that solvents reduce the strength of the cation−π interactions, but the off-axis configurations can still be attractive.

Because of the large induction contributions present in cation−π systems, many pairwise potentials currently used for

large-scale simulations are not able to properly describe this type of bonding. It is our hope that the potential curves presented here may be used as valuable data for the calibration of next generation polarizable force fields.

Supporting Information Available: Figures showing potential energy curves, DFT-SAPT decomposition, and comparison of MP2 and SCF to CCSD(T) counterpoise corrected interaction energies. This material is available free of charge via the Internet at http://pubs.acs.org.

References and Notes

(1) Gromiha, M. M.; Santhosh, C.; Ahmad, S. *Biol. Macromol.* **2004**, *34*, 203.
(2) Heginbotham, L.; MacKinnon, R. *Neuron* **1992**, *8*, 483.
(3) Dougherty, D. A. *Science* **1996**, *271*, 163.
(4) Zhong, W.; Gallivan, J. P.; Zhang, Y.; Li, L.; Lester, H. A.; Dougherty, D. A. *Proc. Natl. Acad. Sci. U.S.A.* **1998**, *95*, 12088.
(5) Meadows, E. S.; Wall, S. L. D.; Barbour, L. J.; Gokel, G. W. *J. Am. Chem. Soc.* **2001**, *123*, 3092.
(6) Singh, N. J.; Min, S. K.; Kim, D. Y.; Kim, K. S. *J. Chem. Theory Comput.* **2009**, *5*, 515.
(7) Yuan, X. L.; Cheng, X. L.; Su, X. F. *Int. J. Quantum Chem.* **2009**, *109*, 972.
(8) Hay, B. P.; Bryantsev, V. S. *Chem. Commun. (Cambridge)* **2008**, *21*, 2393.
(9) Katz, C. E.; Ribelin, T.; Withrow, D.; Basseri, Y.; Manukyan, A. K.; Bermudez, A.; Buera, C. G.; Day, V. W.; Powell, D. R.; Poutsma, J. L.; Aube, J. *J. Org. Chem.* **2008**, *73*, 3318.
(10) Wu, R.; McMahon, T. B. *J. Am. Chem. Soc.* **2008**, *130*, 12554.
(11) Kolmann, S.; Chan, B.; Jordan, M. *Chem. Phys. Lett.* **2008**, *467*, 126.
(12) Mishra, B. K.; Bajpai, V. K.; Ramanathan, V.; Gadre, S. R.; Sathyamurthy, N. *Mol. Phys.* **2008**, *106*, 1557.
(13) Soteras, I.; Orozco, M.; Luque, F. J. *Phys. Chem. Chem. Phys.* **2008**, *10*, 2616.
(14) Tsuzuki, S.; Mikami, M.; Yamada, S. *J. Am. Chem. Soc.* **2007**, *129*, 8656.
(15) Clements, A.; Lewis, M. *J. Phys. Chem. A* **2006**, *110*, 12705.
(16) Pratuangdejkul, J.; Jaudon, P.; Ducrocq, C.; Nosoongnoen, W.; Guerin, G.; Conti, M.; Loric, S.; Launay, J.; Manivet, P. *J. Chem. Theory Comput.* **2006**, *2*, 746.
(17) Reddy, A. S.; Sastry, G. N. *J. Phys. Chem. A* **2005**, *109*, 8893.
(18) Quinonero, D.; Garau, C.; Frontera, A.; Ballester, P.; Costa, A.; Deya, P. *J. Phys. Chem. A* **2005**, *109*, 4632.
(19) Crowley, P. B.; Golovin, A. *Proteins* **2005**, *59*, 231.
(20) Mu, T. W.; Lester, H. A.; Dougherty, D. A. *J. Am. Chem. Soc.* **2003**, *125*, 6850.
(21) Meyer, E. A.; Castellano, R. K.; Diederich, F. *Angew. Chem., Int. Ed.* **2003**, *42*, 1210.
(22) Beene, D. L.; Brandt, G. S.; Zhong, W.; Zacharias, N. M.; Lester, H. A.; Dougherty, D. A. *Biochemistry* **2002**, *41*, 10262.
(23) Amicangelo, J. C.; Armentrout, P. B. *J. Phys. Chem. A* **2000**, *104*, 11420.
(24) Gallivan, J. P.; Dougherty, D. A. *Proc. Natl. Acad. Sci. U.S.A.* **1999**, *96*, 9459.
(25) Feller, D. *Chem. Phys. Lett.* **2000**, *322*, 543.
(26) Minoux, H.; Chipot, C. *J. Am. Chem. Soc.* **1999**, *121*, 10366.
(27) Ma, J. C.; Dougherty, D. A. *Chem. Rev.* **1997**, *97*, 1303.
(28) Mecozzi, S.; West, A. P.; Dougherty, D. A. *J. Am. Chem. Soc.* **1996**, *118*, 2307.
(29) Chipot, C.; Jaffe, R.; Maigret, B.; Pearlman, D. A.; Kollman, P. A. *J. Am. Chem. Soc.* **1996**, *118*, 11217.
(30) Brocchieri, L.; Karlin, S. *Proc. Natl. Acad. Sci. U.S.A.* **1994**, *91*, 9297.
(31) Kearney, P. C.; Mizoue, L. S.; Kumpf, R. A.; Forman, J. E.; McCurdy, A.; Dougherty, D. A. *J. Am. Chem. Soc.* **1993**, *115*, 9907.

(32) Sunner, J.; Nishizawa, K.; Kerbarle, P. *J. Phys. Chem.* **1981**, *85*, 1814.

(33) Tsuzuki, S.; Yoshida, M.; Uchimaru, T.; Mikami, M. *J. Phys. Chem. A* **2001**, *105*, 769.

(34) Armentrout, P. B.; Rodgers, M. T. *J. Phys. Chem. A* **2000**, *104*, 2238.

(35) Feller, D.; Dixon, D. A.; Nicholas, J. B. *J. Phys. Chem. A* **2000**, *104*, 11414.

(36) Woolf, T. B.; Grossfield, A.; Pearson, J. G. *Int. J. Quantum Chem.* **1999**, *75*, 197.

(37) Amunugama, R.; Rodgers, M. T. *J. Phys. Chem. A* **2002**, *106*, 5529.

(38) Amunugama, R.; Rodgers, M. T. *J. Phys. Chem. A* **2002**, *106*, 9718.

(39) Dunbar, R. C. *J. Phys. Chem. A* **2002**, *106*, 7328.

(40) Cheng, Y.-H.; Liu, L.; Fu, Y.; Chen, R.; Li, X.-S.; Guo, Q.-X. *J. Phys. Chem. A* **2002**, *106*, 11215.

(41) Raghavachari, K.; Trucks, G. W.; Pople, J. A.; Head-Gordon, M. *Chem. Phys. Lett.* **1989**, *157*, 479.

(42) Krishnan, R.; Binkley, J. S.; Seeger, R.; Pople, J. A. *J. Chem. Phys.* **1980**, *72*, 650.

(43) McLean, A. D.; Chandler, G. S. *J. Chem. Phys.* **1980**, *72*, 5639.

(44) Blaudeau, J. P.; McGrath, M. P.; Curtiss, L. A.; Radom, L. *J. Chem. Phys.* **1997**, *107*, 5016.

(45) Boys, S. F.; Bernardi, F. *Mol. Phys.* **1970**, *19*, 553.

(46) Gauss, J.; Stanton, J. F. *J. Phys. Chem. A* **2000**, *104*, 2865.

(47) Werner, H. J.; Knowles, P. J.; Lindh, R.; Manby, F. R.; Schütz, M.; Celani, P.; Korona, T.; Rauhut, G.; Amos, R. D.; Bernhardsson, A.; Berning, A.; Cooper, D. L.; Deegan, M. J. O.; Dobbyn, A. J.; Eckert, F.; Hampel, C.; Hetzer, G.; Lloyd, A. W.; McNicholas, S. J.; Meyer, W.; Mura, M. E.; Nicklass, A.; Palmieri, P.; Pitzer, R.; Schumann, U.; Stoll, H.; Stone, A. J.; Tarroni, R.; Thorsteinsson, T. Molpro, version 2006.1, a package of ab initio programs, 2006; see http://www.molpro.net.

(48) Jansen, G.; Hesselmann, A. *J. Chem. Phys. A* **2001**, *105*, 646.

(49) Jeziorski, B.; Moszynski, R.; Szalewicz, K. *Chem. Rev.* **1994**, *94*, 1887.

(50) Williams, H. L.; Szalewicz, K.; Jeziorski, B.; Moszynski, R.; Rybak, S. *J. Chem. Phys.* **1993**, *98*, 1279.

(51) Hesselmann, A.; Jansen, G. *Phys. Chem. Chem. Phys.* **2003**, *122*, 5010.

(52) Hesselmann, A.; Jansen, G. *J. Phys., Lett.* **2002**, *357*, 464.

(53) Hesselmann, A.; Jansen, G. *J. Phys., Lett.* **2002**, *362*, 319.

(54) Hesselmann, A.; Jansen, G. *J. Phys., Lett.* **2003**, *367*, 778.

(55) Grüning, M.; Gritsenko, O. V.; van Gisbergen, S. J. A.; Baerends, E. J. *J. Chem. Phys.* **2001**, *114*, 652.

(56) Cohen, E. R.; Taylor, B. N. *J. Phys. Chem. Ref. Data* **1988**, *17*, 1795.

(57) Lias, S. G. *J. Phys. Chem. Ref. Data* **1988**, 17.

(58) Adamo, C.; Scuseria, G. E.; Barone, V. *J. Chem. Phys.* **1999**, *111*, 2889.

(59) Hohenstein, E. G.; Sherrill, C. D. *J. Phys. Chem. A* **2009**, *113*, 878.

(60) Miertus, S.; Scrocco, E.; Tomasi, J. *Chem. Phys.* **1981**, *55*, 117.

(61) Tomasi, J.; Persico, M. *Chem. Rev.* **1994**, *94*, 2027.

(62) Cammi, R.; Tomasi, J. *J. Comput. Chem.* **1995**, *16*, 1449.

(63) Romasi, J.; Mennucci, B.; Cammi, R. *Chem. Rev.* **2005**, *105*, 2999.

(64) Becke, A. D. *J. Chem. Phys.* **1993**, *98*, 5642.

(65) Schmidt, M. W.; Baldridge, K. K.; Boatz, J. A.; Elbert, S. T.; Gordon, M. S.; Jensen, J. J.; Koseki, S.; Matsunaga, N.; Nguyen, K. A.; Su, S.; Windus, T. L.; Dupuis, M.; Montgomery, J. A. *J. Comput. Chem.* **1993**, *14*, 1347.

(66) Nakamura, H.; Sakamoto, T.; Wada, A. *Protein Eng.* **1988**, *2*, 177.